Power Grid Probing for Load Learning: Identifiability over Multiple Time Instances

Siddharth Bhela and Vassilis Kekatos
ECE Dept., Virginia Tech,
Blacksburg, VA 24061, USA

Sriharsha Veeramachaneni
WindLogics Inc.,
St Paul, MN 55108, USA

***Abstract*—Although nodal loads and renewable generation need to be known for solving different grid optimization tasks, power distribution networks currently lack extensive metering infrastructure. The fresh idea here is to exploit the capabilities of smart inverters found in solar panels and energy storage devices to probe the grid and thus infer the power injections at non-metered nodes. Probing can be accomplished by commanding inverters to change their active injections and power factors momentarily, and subsequently record the incurred voltages as responses of the underlying physical system. Load inference via grid probing boils down to an implicit nonlinear system identification task and involves solving a sequence of power flow problems coupled over multiple probing periods. Invoking results from structured control, an intuitive rule pertaining to the locations of metered and non-metered nodes on the grid graph is shown to be sufficient for ensuring local identifiability in radial and meshed networks. The identifiability criterion scales favorably over time and is numerically corroborated on the IEEE 34-bus feeder.**

***Index Terms*—Smart inverters, power flow problem, Jacobian matrix, graph Laplacian, generic rank, structural observability.**

I. Introduction

With the integration of renewables, electric vehicles, and demand-response programs, there is an urging need for solving optimization tasks in power distribution grids. Optimal control and resource allocation in power grids however requires knowing precisely the non-controllable power injections at all network nodes. Although only a few buses are currently metered frequently enough, the power inverters found in solar panels, electric vehicles, and batteries, with their advanced actuation, sensing, and communication capabilities, constitute an excellent opportunity for learning non-metered loads.

Nodal power injections can be calculated once the power system state, that is the complex voltages across all nodes, is known. Given noiseless specifications, the latter task constitutes the widely studied *power flow* (PF) problem involving a set of non-linear equations [1], [2], [3]. The existence and uniqueness of PF solutions as well as devising PF solvers are active research areas [4], [5], [6], [7]. Providing two specifications per node though may be unrealistic in current distribution grids. Under a noisy setup, the system state can be inferred through state estimation presuming the set of grid data is sufficiently rich [8], [9], [10]. A kernel-based load learning scheme ignoring network information is suggested in [11]. Under an approximate grid model, conditions under which smart meter data from a subset of nodes can be used to infer non-metered loads are developed in [12].

The aforementioned approaches passively collect data to infer loads. This work builds on the idea of *grid probing* for load inference as introduced in [13]. Probing, that is intentionally perturbing a power system to infer unknown parameters, has been advocated in [14] and [15] for estimating the oscillation modes of high-voltage power transmission systems. Moreover, modulating the primary droop control loop of inverters for learning direct-current microgrids has been suggested in [16].

This work extends our previous work in [13] in two fronts. First, we provide intuitive and easily verifiable graph-theoretic conditions under which probing over multiple time slots can successfully recover unmonitored loads. The conditions capture the effects of the number of probing actions and the topological setup between actuated and non-metered loads. Second, a new proving technique generalizes our results from radial to meshed grids, thus covering the timely topic of loopy multiphase distribution grids as well as transmission systems.

Notation: Column vectors (matrices) are denoted by lower- (upper-) case boldface letters; sets by calligraphic symbols; while $|\mathcal{X}|$ is the cardinality of set $\mathcal{X}$. The operator $(\cdot)^\top$ stands for transposition; $\mathrm{d}(\mathbf{x})$ defines a diagonal matrix having $\mathbf{x}$ on its main diagonal; and $\mathrm{rank}(\cdot)$ is the matrix rank. The notation $\mathbf{x}_\mathcal{A}$ means the sub-vector of $\mathbf{x}$ indexed by the set $\mathcal{A}$, while $\mathbf{X}_{\mathcal{A},\mathcal{B}}$ is the matrix obtained by sampling the rows and columns of $\mathbf{X}$ indexed by subsets $\mathcal{A}$ and $\mathcal{B}$.

II. Multi-Instance Grid Probing

Before presenting our learning approach, let us briefly review a grid model and the related PF equations. A power network having $N+1$ nodes can be represented by a graph $\mathcal{G} = (\mathcal{N}^+, \mathcal{L})$, whose nodes $\mathcal{N}^+ := \{0, \ldots, N\}$ correspond to buses, and edges $\mathcal{L}$ to distribution lines. The substation bus is indexed by $n = 0$ and the remaining buses comprise set $\mathcal{N}$. The voltage phasor at bus n is expressed in rectangular coordinates as $v_{r,n} + jv_{i,n}$. The $2(N+1)$–length vector collecting the rectangular coordinates of all nodal voltage phasors, namely $\mathbf{v} := [\mathbf{v}_r^\top \ \mathbf{v}_i^\top]^\top$ with $\mathbf{v}_r := [v_{r,0} \ \ldots \ v_{r,N}]^\top$ and $\mathbf{v}_i := [v_{i,0} \ \ldots \ v_{i,N}]^\top$, constitutes the system state.

Let $\mathbf{Y} := \mathbf{G} + j\mathbf{B}$ denote the system bus admittance matrix with $\mathbf{G}$ and $\mathbf{B}$ being the Laplacian matrices of the grid graph $\mathcal{G}$ weighted respectively by the line conductances and

The work of S. Bhela was supported by a grant from Windlogics Inc.

reactances [17, Ch. 3], [18]. By definition, the entries B_{nm} and G_{nm} for $n \neq m$ are non-zero only if buses n and m are physically connected. The active and reactive power injections at bus n can be expressed as quadratic functions of $\mathbf{v}$ as $p_n(\mathbf{v}) = v_{r,n}\sum_{m=1}^N (v_{r,m}G_{nm} - v_{i,m}B_{nm}) + v_{i,n}\sum_{m=1}^N (v_{i,m}G_{nm} + v_{r,m}B_{nm})$ and $q_n(\mathbf{v}) = v_{i,n}\sum_{m=1}^N (v_{r,m}G_{nm} - v_{i,m}B_{nm}) - v_{r,n}\sum_{m=1}^N (v_{i,m}G_{nm} + v_{r,m}B_{nm})$, accordingly. The squared voltage magnitude at bus n is a quadratic function of $\mathbf{v}$ as well since $u_n(\mathbf{v}) = v_{r,n}^2 + v_{i,n}^2$.

In the conventional PF problem, the system operator fixes two out of the three quantities (u_n, p_n, q_n) for each bus $n \in \mathcal{N}$ to specified values along with $v_{r,0} + jv_{i,0} = 1$ for the substation, and solves (locally) the related nonlinear PF equations to recover $\mathbf{v}$ [17, Ch. 3]. Although the requirement of knowing two out of the three quantities is typically met in transmission systems, that is hardly the case in distribution grids due to limited metering and communication infrastructure [19].

On the other hand, with the proliferation of smart meters and smart inverters, the grid operator may have access to all three quantities (u_n, p_n, q_n) on a subset of buses. Different from the classic PF setup, let us partition $\mathcal{N}^+$ into two subsets:

- The set $\mathcal{M}$ of metered nodes for which (u_n, p_n, q_n) are known and injections are possibly controllable. This set includes the substation and nodes equipped with meters and/or smart inverters.
- The remaining set $\mathcal{O}$ of non-metered nodes where no information is available.

If $|\mathcal{M}| = M$ and $|\mathcal{O}| = O$, it follows that $M + O = N + 1$.

At time t and given the grid data $\{(u_n^t, p_n^t, q_n^t)\}_{n\in\mathcal{M}}$, the system operator could try recovering the unknown loads in $\mathcal{O}$ by first finding the unknown system state $\mathbf{v}_t$ and then substituting $\mathbf{v}_t$ into $\{p_n(\mathbf{v}_t), q_n(\mathbf{v}_t)\}_{n\in\mathcal{O}}$. Finding $\mathbf{v}_t$ entails solving the set of nonlinear equations

$$u_n(\mathbf{v}_t) = u_n^t, \qquad \forall n \in \mathcal{M} \tag{1a}$$
$$p_n(\mathbf{v}_t) = p_n^t, \qquad \forall n \in \mathcal{M} \tag{1b}$$
$$q_n(\mathbf{v}_t) = q_n^t, \qquad \forall n \in \mathcal{M}. \tag{1c}$$

To waive the phase ambiguity in voltage phasors, the substation voltage angle is arbitrarily set to zero, thus adding $v_{i,0} = 0$ in the equation set of (1). By a simple count of the number of unknowns and equations, a necessary condition for solving (1) is that $3M + 1 \geq 2(N + 1)$ or $M \geq 2O - 1$, that is the number of metered buses must be at least twice the number of non-metered ones. This condition may be hard to meet either because either there are not sufficiently many metered buses or data cannot be communicated frequently enough.

To relax the condition on M, we propose a *multi-instant coupled power flow* (MCPF) approach. The idea is to couple the specifications related to multiple different system states $\{\mathbf{v}_t\}_{t=1}^T$. The grid transitions from $\mathbf{v}_t$ to $\mathbf{v}_{t+1}$ by intentionally perturbing inverter injections. Smart inverters can be commanded within microseconds to curtail their active power or change their power factor for one second, and then return to their initial status. After each probing action, the grid converges promptly to a new steady state which nevertheless depends on the non-perturbed injections as well. Grid probing can be repeated T successive slots indexed by $t \in \mathcal{T}$ with $\mathcal{T} := \{1, \ldots, T\}$. Each probing action provides an additional set of equations identical in structure to those in (1).

The sets of equations in (1) for $t \in \mathcal{T}$ are seemingly independent. But if non-metered injections remain unaltered during the probing period, we obtain the additional specifications

$$p_n(\mathbf{v}_t) = p_n(\mathbf{v}_{t+1}), \qquad \forall n \in \mathcal{O}, t = 1, \ldots, T-1 \tag{2a}$$
$$q_n(\mathbf{v}_t) = q_n(\mathbf{v}_{t+1}), \qquad \forall n \in \mathcal{O}, t = 1, \ldots, T-1 \tag{2b}$$

that couple system states across $\mathcal{T}$. The MCPF task can be now formally stated as follows.

Definition 1 (MCPF task)**.** *Given the grid admittance matrix* $\mathbf{Y}$ *and grid data* $\{(u_n^t, p_n^t, q_n^t)\}_{n\in\mathcal{M},t\in\mathcal{T}}$*, the multi-instance coupled power flow problem entails solving the equations in* (1) *for* $t \in \mathcal{T}$ *jointly with the coupling equations in* (2)*.*

The total number of equations in (1) is $(3M + 1)T$, while the coupling equations in (2) is $2O(T - 1)$. Since the total number of variables is $2(M + O)T$, a necessary condition for solving MCPF is $M \geq \frac{2O}{T} - 1$, which improves upon the single-slot condition of $M \geq 2O - 1$. But is this condition sufficient for solving the MCPF problem? The next section studies the identifiability of MCPF.

III. Identifiability Analysis

MCPF can be interpreted as a nonlinear system identification problem where the perturbed injections $\{p_n^t, q_n^t\}_{n\in\mathcal{M},t\in\mathcal{T}}$ are the inputs, the metered voltage magnitudes $\{u_n^t\}_{n\in\mathcal{M},t\in\mathcal{T}}$ are the outputs, and the time-invariant non-metered injections $\{p_n, q_n\}_{n\in\mathcal{O}}$ are the sought system variables. As customary in identifiability analysis, data will be assumed noiseless; noisy counterparts of MCPF are considered in [20].

The MCPF input-output relationship is implicit since the PF equations involve $\{\mathbf{v}_t\}$ as nuisance variables. Because of this, MCPF is tackled in two steps. The first step of finding $\{\mathbf{v}_t\}$ is the challenging one. The second step simply evaluates $\{p_n(\mathbf{v}_1), q_n(\mathbf{v}_1)\}_{n\in\mathcal{O}}$. Hence, if the system states $\{\mathbf{v}_t\}$ are identifiable through (1)–(2), MCPF is deemed successful.

Since the MCPF equations are non-linear, identifiability can be guaranteed only within a neighborhood of the nominal $\{\mathbf{v}_t\}$. According to the inverse function theorem, a necessary and sufficient condition for locally solving MCPF is that the Jacobian matrix $\mathbf{J}(\{\mathbf{v}_t\})$ related to the functions in (1)–(2) is full column rank. Due to the nonlinearity, matrix $\mathbf{J}(\{\mathbf{v}_t\})$ apparently depends on the system state values. Because characterizing the column rank of $\mathbf{J}(\{\mathbf{v}_t\})$ for any $\{\mathbf{v}_t\}$ is challenging, we resort to the concept of the generic rank of a matrix. The identifiability of MCPF is analyzed after introducing the tool of structural identifiability.

The *generic rank* of a matrix has been widely used in observability and controllability of linear dynamical systems [21]. It is defined as the maximum possible (column) rank attained if the non-zero entries of the matrix are allowed to take arbitrary values in $\mathbb{R}$. Thus, the generic rank of a matrix depends only on its sparsity pattern. Apparently, the sparsity pattern of $\mathbf{J}(\{\mathbf{v}_t\})$ cannot adequately capture its column rank. Even in the conventional PF setup, there exist specification sets for which the related Jacobian matrix is invertible in general, though it becomes singular under specific state values (including the boundaries for voltage collapse); see e.g., [17].

The generic rank relates to a graph defined by the sparsity pattern of the matrix. To explain this link, some definitions from graph theory are needed. A graph is *bipartite* if its vertex set $\mathcal{V}$ can be partitioned into two mutually exclusive and collectively exhaustive subsets $\mathcal{V}_1$ and $\mathcal{V}_2$, such that every edge $e \in \mathcal{E}$ connects a node in $\mathcal{V}_1$ with a node in $\mathcal{V}_2$. Moreover, a *matching* $\mathcal{E}' \subseteq \mathcal{E}$ is a subset of edges so that each node in $\mathcal{V}$ is adjacent to at most one edge in $\mathcal{E}'$. A matching is *perfect* if each node in $\mathcal{V}$ has exactly one edge in $\mathcal{E}'$ incident to it.

Let us associate matrix $\mathbf{E} \in \mathbb{R}^{M\times N}$ with a bipartite graph $\mathcal{G}_E$ having $M+N$ nodes. Each column of $\mathbf{E}$ is mapped to a column node, and each row of $\mathbf{E}$ to a row node. An edge runs from the n-th column node to the m-th row node only if $E_{mn} \neq 0$. Based on $\mathcal{G}_E$, the ensuing result holds [22].

Lemma 1 ([22])**.** *Matrix $\mathbf{E}$ has full generic column rank if and only if the bipartite graph $\mathcal{G}_E$ exhibits a perfect matching from the column nodes to its row nodes.*

From Lemma 1, the generic identifiability of MCPF relies on the sparsity pattern of $\mathbf{J}(\{\mathbf{v}_t\})$. The goal is to match every column node of $\mathbf{J}(\{\mathbf{v}_t\})$ to a unique row node. The non-zero entries of $\mathbf{J}(\{\mathbf{v}_t\})$ designate the available links. Recall that its columns correspond to state variables $v_{r,n}^t$ or $v_{i,n}^t$ for $n \in \mathcal{N}^+$ and $t \in \mathcal{T}$, while its rows relate to the equations in (1)–(2).

The MCPF task can be equivalently expressed as the problem of solving the nonlinear equations $\mathbf{h}(\{\mathbf{v}_t\}) = \mathbf{0}$ where the mapping $\mathbf{h}: \mathbb{R}^{2(N+1)T} \rightarrow \mathbb{R}^{(3M+1)T+2O(T-1)}$ stacks the equations in (1)–(2). To find the related Jacobian matrix, define the mappings from $\mathbf{v}$ to the vectors of squared voltage magnitudes and power injections at all buses

$$\mathbf{u}(\mathbf{v}) := [u_0(\mathbf{v}) \ \dots \ u_N(\mathbf{v})]^\top \tag{3a}$$
$$\mathbf{p}(\mathbf{v}) := [p_0(\mathbf{v}) \ \dots \ p_N(\mathbf{v})]^\top \tag{3b}$$
$$\mathbf{q}(\mathbf{v}) := [q_0(\mathbf{v}) \ \dots \ q_N(\mathbf{v})]^\top. \tag{3c}$$

Nodal power injections are defined as $\mathbf{p}+j\mathbf{q} = \mathrm{d}(\mathbf{v})\mathbf{i}^*$ with $\mathbf{i} = \mathbf{Y}\mathbf{v}$ being the vector of nodal currents. Eliminating $\mathbf{i}$ yields $\mathbf{p}+j\mathbf{q} = \mathrm{d}(\mathbf{v})\mathbf{Y}^*\mathbf{v}^*$. By transforming these equations to their rectangular coordinates and differentiating, the Jacobian matrices for the mappings in (3) can be shown to be [6]

$$\mathbf{J}^u(\mathbf{v}) = \begin{bmatrix} 2\,\mathrm{d}(\mathbf{v}_r) & 2\,\mathrm{d}(\mathbf{v}_i) \end{bmatrix} \tag{4a}$$
$$\mathbf{J}^p(\mathbf{v}) = \begin{bmatrix} -\mathbf{G}\,\mathrm{d}(\mathbf{v}_r) - \mathbf{B}\,\mathrm{d}(\mathbf{v}_i) & -\mathbf{G}\,\mathrm{d}(\mathbf{v}_i) + \mathbf{B}\,\mathrm{d}(\mathbf{v}_r) \\ -\mathrm{d}(\mathbf{G}\mathbf{v}_r) + \mathrm{d}(\mathbf{B}\mathbf{v}_i) & -\mathrm{d}(\mathbf{B}\mathbf{v}_r) - \mathrm{d}(\mathbf{G}\mathbf{v}_i) \end{bmatrix} \tag{4b}$$
$$\mathbf{J}^q(\mathbf{v}) = \begin{bmatrix} \mathbf{B}\,\mathrm{d}(\mathbf{v}_r) - \mathbf{G}\,\mathrm{d}(\mathbf{v}_i) & \mathbf{B}\,\mathrm{d}(\mathbf{v}_i) + \mathbf{G}\,\mathrm{d}(\mathbf{v}_r) \\ +\mathrm{d}(\mathbf{B}\mathbf{v}_r) + \mathrm{d}(\mathbf{G}\mathbf{v}_{t,i}) & -\mathrm{d}(\mathbf{G}\mathbf{v}_r) + \mathrm{d}(\mathbf{B}\mathbf{v}_i) \end{bmatrix} \tag{4c}$$

Neglecting the particular matrix entry values, the sparsity pattern of $\mathbf{J}^u(\mathbf{v})$ is captured by $[\mathbf{I}_{N+1}\ \mathbf{I}_{N+1}]$. Matrices $\mathbf{J}^p(\mathbf{v})$ and $\mathbf{J}^q(\mathbf{v})$ have the same sparsity pattern that can be depicted in a simpler form via one of the grid Laplacians as $[\mathbf{B}\ \mathbf{B}]$.

The block partitions of the MCPF Jacobian $\mathbf{J}$ constitute row-sampled submatrices of $\mathbf{J}^u(\mathbf{v}_t)$, $\mathbf{J}^p(\mathbf{v}_t)$, and $\mathbf{J}^q(\mathbf{v}_t)$ for all t. The matrix obtained by preserving the rows of $\mathbf{J}^p(\mathbf{v}_t)$ associated with $\mathcal{M}$ (resp. $\mathcal{O}$) is denoted by $\mathbf{J}^p_{\mathcal{M}}(\mathbf{v}_t)$ (resp. $\mathbf{J}^p_{\mathcal{O}}(\mathbf{v}_t)$). Similar notation is used for $\mathbf{J}^u(\mathbf{v}_t)$ and $\mathbf{J}^q(\mathbf{v}_t)$. Then, matrix $\mathbf{J}(\{\mathbf{v}_t\})$ can be partitioned as

$$\begin{bmatrix}
\mathbf{J}_{\mathcal{M}}(\mathbf{v}_1) & \mathbf{0} & \mathbf{0} & \cdots & \mathbf{0} \\
\mathbf{0} & \mathbf{J}_{\mathcal{M}}(\mathbf{v}_2) & \mathbf{0} & \cdots & \mathbf{0} \\
\mathbf{0} & \mathbf{0} & \mathbf{J}_{\mathcal{M}}(\mathbf{v}_3) & \vdots & \mathbf{0} \\
\vdots & \vdots & \vdots & \ddots & \vdots \\
\mathbf{0} & \mathbf{0} & \mathbf{0} & \cdots & \mathbf{J}_{\mathcal{M}}(\mathbf{v}_T) \\
\hline
\mathbf{J}_{\mathcal{O}}(\mathbf{v}_1) & -\mathbf{J}_{\mathcal{O}}(\mathbf{v}_2) & \mathbf{0} & \cdots & \mathbf{0} \\
\mathbf{0} & \mathbf{J}_{\mathcal{O}}(\mathbf{v}_2) & -\mathbf{J}_{\mathcal{O}}(\mathbf{v}_3) & \cdots & \mathbf{0} \\
\vdots & \vdots & \ddots & \ddots & \vdots \\
\mathbf{0} & \mathbf{0} & \mathbf{0} & \cdots & -\mathbf{J}_{\mathcal{O}}(\mathbf{v}_T)
\end{bmatrix} \tag{5}$$

with the two types of blocks defined as

$$\mathbf{J}_{\mathcal{M}}(\mathbf{v}_t) := \begin{bmatrix} 2\mathbf{e}_{N+2}^\top \\ \mathbf{J}^u_{\mathcal{M}}(\mathbf{v}_t) \\ \mathbf{J}^p_{\mathcal{M}}(\mathbf{v}_t) \\ \mathbf{J}^q_{\mathcal{M}}(\mathbf{v}_t) \end{bmatrix} \quad \text{and} \quad \mathbf{J}_{\mathcal{O}}(\mathbf{v}_t) := \begin{bmatrix} \mathbf{J}^p_{\mathcal{O}}(\mathbf{v}_t) \\ \mathbf{J}^q_{\mathcal{O}}(\mathbf{v}_t) \end{bmatrix}$$

where $\mathbf{e}_{N+2}$ is the $(N+2)$-th canonical vector of length $2(N+1)$. Each $\mathbf{J}_{\mathcal{M}}(\mathbf{v}_t)$ block is of dimension $(3M+1)\times 2(N+1)$ and each $\mathbf{J}_{\mathcal{O}}(\mathbf{v}_t)$ block is $2O \times 2(N+1)$.

The rows of $\mathbf{J}(\{\mathbf{v}_t\})$ associated with the coupling equations can be interlaced with the block rows associated with the single-slot equations such that the resultant row-permuted version of $\mathbf{J}(\{\mathbf{v}_t\})$ denoted by $\tilde{\mathbf{J}}(\{\mathbf{v}_t\})$ is block-tridiagonal

$$\tilde{\mathbf{J}}(\{\mathbf{v}_t\}) = \begin{bmatrix}
\tilde{\mathbf{J}}_1(\mathbf{v}_1) & \cdots & \cdots & \mathbf{0} \\
\vdots & \tilde{\mathbf{J}}_2(\mathbf{v}_2) & \cdots & \cdots \\
\mathbf{0} & \vdots & \ddots & \cdots \\
\mathbf{0} & \mathbf{0} & \vdots & \tilde{\mathbf{J}}_T(\mathbf{v}_T)
\end{bmatrix}. \tag{6}$$

The $2O(T-1)$ coupling equations can be evenly distributed over the T slots. Then, the blocks $\{\tilde{\mathbf{J}}_t(\mathbf{v}_t)\}$ on the main diagonal of $\tilde{\mathbf{J}}(\{\mathbf{v}_t\})$ are of dimension $\left(3M+1+\frac{2O(T-1)}{T}\right) \times 2(N+1)$. If each one of these blocks enjoys a bipartite matching, $\tilde{\mathbf{J}}(\{\mathbf{v}_t\})$ and hence $\mathbf{J}(\{\mathbf{v}_t\})$ are generically full column rank by Lemma 1. In this case, the blocks lying on the super- and sub-diagonals of $\tilde{\mathbf{J}}(\{\mathbf{v}_t\})$ can be ignored.

While designing $\{\tilde{\mathbf{J}}_t(\mathbf{v}_t)\}_{t\in\mathcal{T}}$, an equation coupling slots t and $t+1$ can be assigned to $\tilde{\mathbf{J}}_t(\mathbf{v}_t)$ or $\tilde{\mathbf{J}}_{t+1}(\mathbf{v}_{t+1})$. In [20], we show that this assignment can be accomplished in a way such that each $\tilde{\mathbf{J}}_t(\mathbf{v}_t)$ gets O coupling (active or reactive power) equations covering the entire set $\mathcal{O}$. Each $\tilde{\mathbf{J}}_t(\mathbf{v}_t)$ receives $\frac{O(T-2)}{T}$ *additional* coupling equations related to a subset of nodes $\mathcal{O}_t \subset \mathcal{O}$. The sparsity pattern of $\tilde{\mathbf{J}}_t(\mathbf{v}_t)$ is then

$$\begin{bmatrix}
\mathbf{I}_{\mathcal{M},\mathcal{N}^+} & \mathbf{I}_{\mathcal{M},\mathcal{N}^+} \\
\mathbf{B}_{\mathcal{M},\mathcal{N}^+} & \mathbf{B}_{\mathcal{M},\mathcal{N}^+} \\
\mathbf{B}_{\mathcal{M},\mathcal{N}^+} & \mathbf{B}_{\mathcal{M},\mathcal{N}^+} \\
\mathbf{B}_{\mathcal{O},\mathcal{N}^+} & \mathbf{B}_{\mathcal{O},\mathcal{N}^+} \\
\mathbf{B}_{\mathcal{O}_t,\mathcal{N}^+} & \mathbf{B}_{\mathcal{O}_t,\mathcal{N}^+}
\end{bmatrix} \tag{7}$$

where the first block row relates to metered voltage magnitudes; the second and third block rows to metered injections; while the fourth and fifth block rows to coupled injections.

To create a bipartite matching for block $\tilde{\mathbf{J}}_t(\mathbf{v}_t)$, unfold the sparsity pattern in (7) column-wise using $\mathcal{N}^+ = \mathcal{M} \cup \mathcal{O}$ as

$$\begin{bmatrix} \boxed{\mathbf{I}_{\mathcal{M},\mathcal{M}}} & \mathbf{I}_{\mathcal{M},\mathcal{O}} & \mathbf{I}_{\mathcal{M},\mathcal{M}} & \mathbf{I}_{\mathcal{M},\mathcal{O}} \\ \mathbf{B}_{\mathcal{M},\mathcal{M}} & \mathbf{B}_{\mathcal{M},\mathcal{O}} & \boxed{\mathbf{B}_{\mathcal{M},\mathcal{M}}} & \mathbf{B}_{\mathcal{M},\mathcal{O}} \\ \mathbf{B}_{\mathcal{M},\mathcal{M}} & \mathbf{B}_{\mathcal{M},\mathcal{O}} & \mathbf{B}_{\mathcal{M},\mathcal{M}} & \mathbf{B}_{\mathcal{M},\mathcal{O}} \\ \mathbf{B}_{\mathcal{O},\mathcal{M}} & \boxed{\mathbf{B}_{\mathcal{O},\mathcal{O}}} & \mathbf{B}_{\mathcal{O},\mathcal{M}} & \mathbf{B}_{\mathcal{O},\mathcal{O}} \\ \mathbf{B}_{\mathcal{O}_t,\mathcal{M}} & \mathbf{B}_{\mathcal{O}_t,\mathcal{O}} & \mathbf{B}_{\mathcal{O}_t,\mathcal{M}} & \mathbf{B}_{\mathcal{O}_t,\mathcal{O}} \end{bmatrix}. \tag{8}$$

The first block column in (8) is associated with variables $\{v_{r,n}^t\}_{n\in\mathcal{M}}$ and it can be matched to the first block row via the diagonal of $\mathbf{I}_{\mathcal{M},\mathcal{M}}$. Similarly, the second block column (variables $\{v_{r,n}^t\}_{n\in\mathcal{O}}$) can be matched to the fourth block row; and the third block column (variables $\{v_{i,n}^t\}_{n\in\mathcal{M}}$) can be matched to the second block row.

To complete a bipartite matching, the fourth block column (variables $\{v_{i,n}\}_{n\mathcal{O}}$) has to be matched to the union of the third and fifth block rows. Lacking a simple diagonal matching now, we leverage the sparsity pattern of $\mathbf{B}$ capturing the grid topology. It suffices to match the nodes in $\mathcal{O}$ to the nodes in $\mathcal{M} \cup \mathcal{O}_t$. Because $\mathcal{O} = \mathcal{O}_t \cup \bar{\mathcal{O}}_t$, the nodes in $\mathcal{O}_t$ can be matched to themselves (through some diagonal entries of $\mathbf{B}_{\mathcal{O}_t,\mathcal{O}}$). We are left with having to match the nodes in $\bar{\mathcal{O}}_t$ to the nodes in $\mathcal{M}$. Since $|\mathcal{O}_t| = \frac{O(T-2)}{T}$, it follows $|\bar{\mathcal{O}}_t| = \frac{2O}{T}$.

In summary, to guarantee that $\mathbf{J}(\{\mathbf{v}_t\})$ is generically full column rank, we have to match each subset $\bar{\mathcal{O}}_t$ independently over $t \in \mathcal{T}$ to $\mathcal{M}$. Devising $T/2$ instead of T matchings is actually sufficient as asserted by the next result shown in [20].

Lemma 2. *For even T, the diagonal blocks $\{\tilde{\mathbf{J}}_t(\mathbf{v}_t)\}_{t\in\mathcal{T}}$ in* (6) *exhibit only $T/2$ distinct sparsity patterns. Specifically, the blocks $\tilde{\mathbf{J}}_t(\mathbf{v}_t)$ and $\tilde{\mathbf{J}}_{t+1}(\mathbf{v}_{t+1})$ for odd t have identical patterns, that is $\bar{\mathcal{O}}_t = \bar{\mathcal{O}}_{t+1}$ for odd t.*

The intuition behind the modulo-2 repetition is that injection equations occur in active-reactive pairs with identical sparsity patterns. Based on the above, the main claim on the identifiability of MCPF follows; see [20] for a proof.

Theorem 1. *Consider the grid graph $\mathcal{G} = (\mathcal{N}^+, \mathcal{L})$ with $\mathcal{N}^+ = \mathcal{M} \cup \mathcal{O}$. If $\mathcal{O}$ can be partitioned into the mutually exclusive and collectively exhaustive sets $\{\bar{\mathcal{O}}_k\}_{k=1}^{T/2}$ such that each one of them independently is perfectly matched to $\mathcal{M}$, the Jacobian matrix $\mathbf{J}(\{\mathbf{v}_t\})$ is generically full column rank.*

Theorem 1 implies that for $T = 2$, the entire $\mathcal{O}$ has to be mapped to $\mathcal{M}$. This was previously shown in [23] using a different technique confined to radial grids. Theorem 1 applies to meshed networks including multiphase grids. The seemingly cumbersome task of matching $\{\bar{\mathcal{O}}_k\}_{k=1}^{T/2}$ to $\mathcal{M}$ can be efficiently performed by properly casting it as a maxflow problem [20]. Theorem 1 suggests also that as T increases, progressively smaller subsets of non-metered nodes need to be mapped to $\mathcal{M}$ improving identifiability as illustrated next.

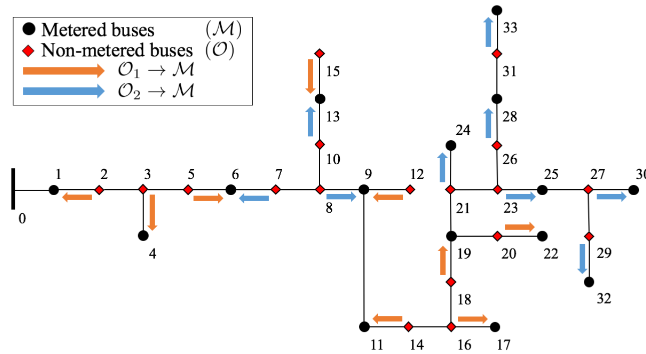

Fig. 1: Matchings on the IEEE 34-bus grid for (T, O)=$(4, 18)$.

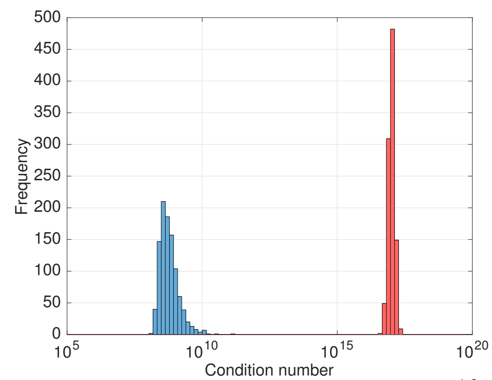

Fig. 2: Condition number histograms for $\mathbf{J}(\{\mathbf{v}_t\})$.

IV. Illustrating Examples

We will use a single-phase equivalent of the IEEE 34-bus feeder [24], [25]. At each zero-injection bus, a load equal to the load of its parent bus was inserted. Solar panels with capacity of 0.1 MVA were considered on all buses in $\mathcal{M}$. Figure 1 depicts a scenario where $O = 18$ out of the 34 buses are non-metered. Probing over $T = 4$ slots is successful, since $\mathcal{O}$ can be partitioned into $\mathcal{O}_1$ and $\mathcal{O}_2$ with 9 buses each, such that they are independently matched to metered buses. Probing over $T = 2$ is not successful though because buses $\{5, 7\}$ for example cannot be uniquely matched to metered ones. Returning to $T = 4$, if buses $\{20, 32\}$ are swapped between $\mathcal{O}$ and $\mathcal{M}$, the criterion of Th. 1 is not met either.

Since Th. 1 relies on the sparsity pattern rather than the exact values of $\mathbf{J}(\{\mathbf{v}_t\})$, we evaluated $\mathbf{J}(\{\mathbf{v}_t\})$ for 1,000 random $\{\mathbf{v}_t\}$. At $t = 1$, the solar panels were assumed to be producing 4 times their active load or 0.1 MW, whichever was smaller. During probing $t \in \{2, 3, 4\}$, solar generation was randomly curtailed in a uniform fashion independently per bus in $\mathcal{M}$. Reactive injections used the remaining inverter apparent capacity with random signs. The histograms for the condition number of $\mathbf{J}(\{\mathbf{v}_t\})$ obtained with and without swapping buses $\{20, 32\}$ are shown in Fig. 2 and comply with Th. 1.

To conclude, this work has put forth multi-period probing for learning non-metered injections. A sufficient identifiability condition has been derived applying to meshed grids and quantifying the benefit of longer probing periods. The effect of noise, efficient solvers, optimal probing design, and graph-imposed bounds on O and T constitute current research topics.

References

[1] W. F. Tinney and C. E. Hart, "Power flow solution by Newton's method," *IEEE Trans. Power App. Syst.*, vol. 86, no. 11, pp. 1449–1460, Nov. 1967.

[2] D. Mehta, D. K. Molzahn, and K. Turitsyn, "Recent advances in computational methods for the power flow equations," in *Proc. IEEE American Control Conf.*, Boston, MA, Jul. 2016.

[3] W. Murray, T. Tinoco De Rubira, and A. Wigington, "A robust and informative method for solving large-scale power flow problems," *Computational Optimization and Applications*, vol. 62, no. 2, pp. 431–475, 2015.

[4] K. Dvijotham, E. Mallada, and J. W. Simpson-Porco, "High-voltage solution in radial power networks: Existence, properties and equivalent algorithms," (submitted 2017). [Online]. Available: https://arxiv.org/pdf/1706.05290.pdf

[5] H. D. Nguyen and K. S. Turitsyn, "Appearance of multiple stable load flow solutions under power flow reversal conditions," in *Proc. IEEE PES General Meeting*, National Harbor, MD, Jul. 2014.

[6] R. Madani, J. Lavaei, and R. Baldick, "Convexification of power flow problem over arbitrary networks," in *Proc. IEEE Conf. on Decision and Control*, Osaka, Japan, Dec. 2015.

[7] M. Bazrafshan and N. Gatsis, "Convergence of the Z-bus method for three-phase distribution load-flow with ZIP loads," *IEEE Trans. Power Syst.*, vol. PP, no. 99, pp. 1–1, 2017.

[8] H. Zhu and G. B. Giannakis, "Power system nonlinear state estimation using distributed semidefinite programming," *IEEE J. Sel. Topics Signal Process.*, vol. 8, no. 6, pp. 1039–1050, Dec. 2014.

[9] C. Klauber and H. Zhu, "Distribution system state estimation using semidefinite programming," in *Proc. North American Power Symposium*, Charlotte, NC, Oct. 2015.

[10] Y. Zhang, R. Madani, and J. Lavaei, "Power system state estimation with line measurements," in *Proc. IEEE Conf. on Decision and Control*, Las Vegas, NV, Dec. 2016.

[11] J. Yu, Y. Weng, and R. Rajagopal, "Mapping rule estimation for power flow analysis in distribution grids," (submitted 2017). [Online]. Available: https://arxiv.org/abs/1702.07948

[12] S. Bhela, V. Kekatos, and S. Veeramachaneni, "Power distribution system observability with smart meter data," in *Proc. IEEE Global Conf. on Signal and Information Process.*, Montreal, Canada, Nov. 2017.

[13] ——, "Enhancing observability in distribution grids using smart meter data," *IEEE Trans. Smart Grid*, vol. PP, no. 99, pp. 1–9, 2017.

[14] N. Zhou, D. J. Trudnowski, J. W. Pierre, and W. Mittelstadt, "Electromechanical mode online estimation using regularized robust RLS methods," *IEEE Trans. Power Syst.*, vol. 23, no. 4, pp. 1670–1680, Nov. 2008.

[15] D. Trudnowski and J. Pierre, "Signal processing methods for estimating small-signal dynamic properties from measured responses," in *Inter-area Oscillations in Power Systems*, ser. Power Electronics and Power Systems, A. R. Messina, Ed. Springer, 2009, pp. 1–36.

[16] M. Angjelichinoski, A. Scaglione, P. Popovski, and C. Stefanovic, "Making the grid truly smart: Autonomous system identification in "modemless" DC microgrids," (submitted 2017). [Online]. Available: https://arxiv.org/pdf/1703.10467.pdf

[17] A. Gómez-Expósito, A. J. Conejo, and C. Canizares, Eds., *Electric Energy Systems, Analysis and Operation*. Boca Raton, FL: CRC Press, 2009.

[18] G. B. Giannakis, V. Kekatos, N. Gatsis, S.-J. Kim, H. Zhu, and B. Wollenberg, "Monitoring and optimization for power grids: A signal processing perspective," *IEEE Signal Processing Mag.*, vol. 30, no. 5, pp. 107–128, Sep. 2013.

[19] G. T. Heydt, "The next generation of power distribution systems," *IEEE Trans. Smart Grid*, vol. 1, no. 3, pp. 225–235, Dec. 2010.

[20] S. Bhela and V. Kekatos, "Distribution network probing for injection inference," (in preparation). [Online]. Available: http://www.faculty.ece.vt.edu/kekatos/papers/TSG17.pdf

[21] J.-M. Dion, C. Commault, and J. van der Woude, "Survey generic properties and control of linear structured systems: A survey," *Automatica*, vol. 39, no. 7, pp. 1125–1144, Jul. 2003.

[22] W. T. Tutte, "The factorization of linear graphs," *Journal of the London Mathematical Society*, vol. 22, no. 2, pp. 107–111, 1947.

[23] S. Bhela, V. Kekatos, L. Zhang, and S. Veeramachaneni, "Enhancing observability in power distribution grids," in *Proc. IEEE Intl. Conf. on Acoustics, Speech, and Signal Process.*, New Orleans, LA, Mar. 2017.

[24] W. H. Kersting, "Radial distribution test feeders," in *Proc. Power Engineering Society Winter Meeting*, vol. 2, 2001, pp. 908–912.

[25] L. Gan, N. Li, U. Topcu, and S. Low, "On the exactness of convex relaxation for optimal power flow in tree networks," in *Proc. IEEE Conf. on Decision and Control*, Maui, HI, Dec. 2012, pp. 465–471.